PERGAMON International Journal of Multiphase Flow 24 (1998) 947–960

International Journal of Multiphase Flow

Flow patterns during boiling in a narrow space between two vertical surfaces

J. Bonjour, M. Lallemand

INSA, CETHIL, UPRES A CNRS 5008, Bât 404 - 20, Av. Albert Einstein - 69621, Villeurbanne Cedex, France

Received 22 July 1997; received in revised form 14 June 1998

Abstract

An experimental study has been carried out in order to identify the different regimes of natural convective boiling of R-113 in a narrow rectangular vertical channel (confined space). The channel height is 120 mm and the gap-size ranges from 0.5 to 2 mm. Three boiling regimes were observed : nucleate boiling with isolated deformed bubbles, nucleate boiling with coalesced bubbles and partial dryout. Both first regimes result in a heat transfer enhancement whereas the latter implies a heat transfer deterioration. The phase detection was achieved by means of the hot-wire anemometry. Based on this method, several parameters such as frequencies and times of bubble passages and void fractions were measured locally. From these measurements, objective criteria are proposed for the transitions between the various regimes. A new flow pattern map for confined boiling, based on the Bond number and a reduced heat flux (ratio of the heat flux to the critical heat flux), has been developed in order to determine the regimes. © 1998 Elsevier Science Ltd. All rights reserved.

Keywords: Pool boiling; Confined space; Narrow channel; Hot-wire anemometry; Void fraction; Flow pattern map

1. Introduction

During recent years, boiling in narrow spaces has become a research subject of great importance as this phenomenon occurs in many practical situations such as plate heat exchangers, motor cooling (Gentile and Zidat, 1992) or electronic component cooling (Jomard et al., 1992). Indeed, when one dimension of the space in which boiling takes places is narrow enough (i.e. when the gap-size is lower than 0.5–5 mm depending on the geometry, the fluid nature, the heat flux, ...), the hydrodynamic characteristics of boiling and heat transfer are very different from those observed in pool boiling. It is now well known from the literature that confined boiling is an efficient heat transfer enhancement technique that can result in heat transfer improvements up to 300%–800% at low heat fluxes, as compared with unconfined

0301-9322/98/$19.00 © 1998 Published by Elsevier Science Ltd. All rights reserved.
PII: S0301-9322(98)00017-2

boiling (Yao and Chang, 1983 ; Xia et al., 1992 ; Rampisela, 1993 ; Bonjour and Lallemand, 1995). However, a deterioration of heat transfer appears at high heat fluxes and the critical heat flux (CHF) is much lower for confined than for unrestricted boiling (Monde et al., 1982 ; Fujita et al., 1988 ; Bonjour and Lallemand, 1997).

The heat transfer enhancement or degradation obviously depends on the confined boiling regimes. Yao and Chang (1983) observed four regimes for confined boiling of water, acetone and R-113 in an annular space ($H = 25.4$ mm or 76.2 mm and 0.32 mm $< e <$ 2.58 mm) whose bottom is closed. The regime of *isolated deformed bubbles* occurs for small gaps and low heat fluxes. Few bubbles having the shape of a half-sphere with a flat bottom are present on the heating wall. For moderate heat fluxes and low gap-sizes, some large vapor plugs, also called *coalesced deformed bubbles*, flow upward along the heating surface. Those two regimes result in a heat transfer enhancement. When the heat flux is close to CHF, Yao and Chang (1983) described the *dryout* regime. For very large gap-sizes and high heat fluxes, *nucleate boiling with slightly deformed bubbles* takes place. This last regime is a mixed condition of pool boiling, characterized by small bubbles, and confined boiling, with coalesced or deformed bubbles.

Xia et al. (1992) observed two regimes for the boiling of R-113 in a rectangular vertical channel ($H = 88$ mm, 0.8 mm $< e <$ 5 mm). When $e > 3$ mm, bubbles are not deformed and the boiling flow pattern is very similar to that of forced convective boiling in vertical tubes. For $e < 3$ mm, adjacent bubbles coalesce and one point of the heating surface is alternately covered with vapor or liquid. However, the boiling flow pattern depends not only on gap-sizes but also on the heating process.

Rampisela (1993) described three regimes for boiling of R-113 in a rectangular vertical channel ($H = 120$ mm, 1 mm $< e <$ 5 mm) between a heated plate and a parallel unheated plate. For low heat fluxes and large gap-sizes, there appears a regime quite similar to unconfined boiling regime called *nucleate boiling with deformed bubbles*. The bubbles are squeezed against the heated wall and have an ellipsoid shape. For moderate heat fluxes and gap-sizes, Rampisela observed a *plug flow* regime, similar to the coalesced bubbles regime visualized by Yao and Chang (1983). The third regime is the *annular flow* that occurs for high heat fluxes and low gap-sizes. In that case, the whole heating plate is covered by a vapor film, which results in heat transfer deterioration. It seems to be identical to the dryout regime observed by Yao and Chang (1983).

Both Rampisela (1993) and Yao and Chang (1983) located the regimes on a flow pattern map based on two dimensionless numbers : the Bond number (Bo) and the Boiling number (Bl). The Bond number is defined as the ratio of the channel gap-size to the departure diameter of isolated bubbles (Yao and Chang, 1983):

$$Bo = e\left(\frac{\sigma}{\boldsymbol{g}(\rho_{\mathrm{L}} - \rho_{\mathrm{G}})}\right)^{-1/2}, \tag{1}$$

where σ is the surface tension, $\boldsymbol{g}$ the gravitational acceleration and ρ_{L} and ρ_{G} the liquid and vapor densities. This number represents the squeezing effect of a bubble due to the confinement. For low Bond numbers (of the order of unity or less), the squeezing effect is important since bubbles cannot grow naturally because the channel is narrower than the bubble diameter. For high Bond numbers, boiling can almost be considered as unconfined.

The Boiling number characterizes the ratio of the time necessary for a bubble to rise along the channel to its time of growth in the gap (Yao and Chang, 1983):

$$Bl = P\frac{qH}{\rho_G h_{LG} eV}, \tag{2}$$

where h_{LG} is the latent heat of vaporization, V the bubble rising velocity and q the heat flux.

Both previous authors proposed an expression for the calculation of the bubble rising velocity for their own geometry. However, these expressions do not take into account the acceleration of the two-phase fluid in the confined space. Bonjour et al. (1996) suggested another expression for this velocity in a rectangular vertical channel, in order to take into account the influence of the channel gap-size on this velocity.

From this literature review, we notice that neither regimes, nor transitions between them have been defined precisely. This may be attributed to a scatter between experimental conditions (fluid, geometry, heating conditions, ...), but overall to the difficulty in identifying regimes from subjective criteria obtained from a visualization by means of photographs, films or the naked eye. That is the reason why the present study will account for the determination of boiling regimes in a rectangular vertical narrow channel on the basis of objective criteria. Those criteria are based on measurements of hydrodynamic characteristics of the two-phase flow, such as void fraction and bubble passage frequency or time, obtained by means of hot-wire anemometry (HWA). Hsu et al. (1963) and Delhaye (1969) have already proposed the use of HWA to analyze the structure of a two-phase flow. Carvalho and Bergles (1991) showed the ability of this technique to provide such information for a two-phase flow during pool boiling. Moreover, Toral (1981) pointed out that hot-wire probes whose diameter is lower than 5 μm result in less perturbations than optical or resistive probes. Herringe and Davis (1974), who compared three phase-discrimination methods (HWA, resistive probes and infra-red absorption systems), recommended the use of HWA when the continuous phase is not an electric conductor. The last objective of this study is to use these criteria in order to establish a new flow pattern map usable to determine the different regimes.

2. Experimental Set-up and Procedure

2.1. Experimental apparatus

The experimental apparatus (Fig. 1) consists of a gas- and liquid tight vessel filled with saturated R-113. A copper block (120 mm high and 60 mm wide), heated by two heaters (1000 W each), is immersed in the fluid. It is thermally insulated on all its faces except on one vertical wall in order to limit the heat losses. According to a numerical simulation for unconfined boiling, heat losses are 8% of the power supplied to the copper block at low heat flux and decrease quickly with increasing heat flux to reach 3% at high heat flux. Moreover, heat losses are lower for confined boiling since the heat transfer coefficient is increased, which implies a lower thermal resistance. That is the reason why these losses are always neglected. At least, because of the high thermal conductivity of copper and because of the large width of the heated surface (60 mm), the isothermal lines are almost parallel to the wall surface (to within

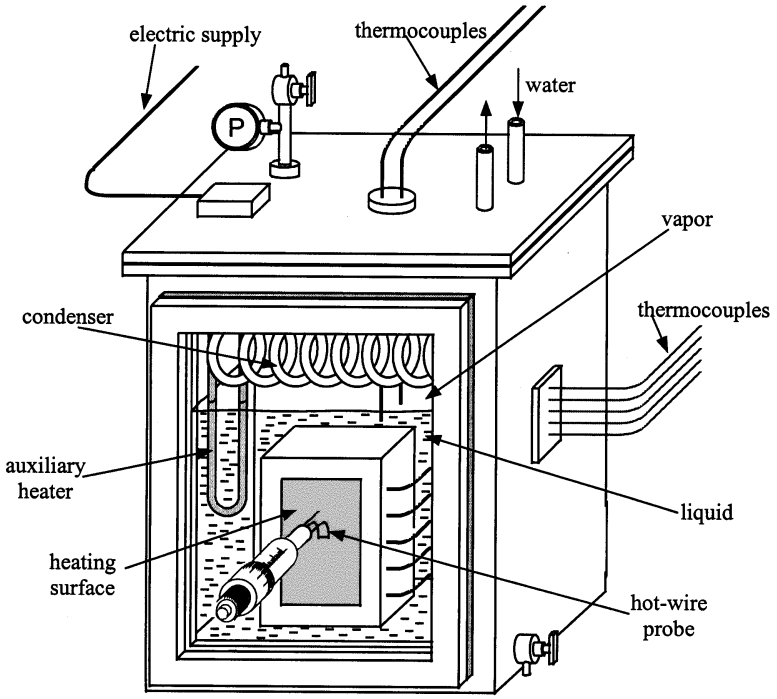

Fig. 1. Schematic of the experimental apparatus.

0.1 K). At the interface between the copper block and the thermal insulant, the isothermal lines are slightly distorted, but it is considered as a side-effect that is not taken into account since all measurements (temperature and HWA measurements) are made along the central vertical axis of the heated wall.

A polycarbonate transparent plate is placed parallel to the heated copper wall to form a rectangular vertical channel whose sides and bottom are left open, so that the fluid mainly enters into the channel from the bottom. The gap-size is accurately set by means of space adjusters whose thickness is 0.3, 0.5, 1 or 2 mm. A distance of 50 mm, which separates the channel base from the base of the fluid container, has been determined by preliminary tests. We have shown that a minimum value of immersion-depth and sidewall distance for the heater must be set to obtain results independent of these parameters, as stated by Westwater et al. (1986) and Elkassabgi and Lienhard (1987). The vapor generated in the channel rises up to the free interface and condenses in a water-cooled condenser. An auxiliary heater is used to keep the fluid at a fixed operating temperature independently of the power supplied to the copper sample.

As regards instrumentation, a pressure gauge is used to ensure that the pressure is kept at 1 bar during all tests. A voltmeter and an ammeter allow the evaluation of the heat flux in the block. Thermocouples are used to measure the temperatures of the liquid and the vapor and some are inserted into the copper block at seven locations (Fig. 2), 0.5 mm from the surface. During experiments, we always verified that the temperature measured by thermocouples

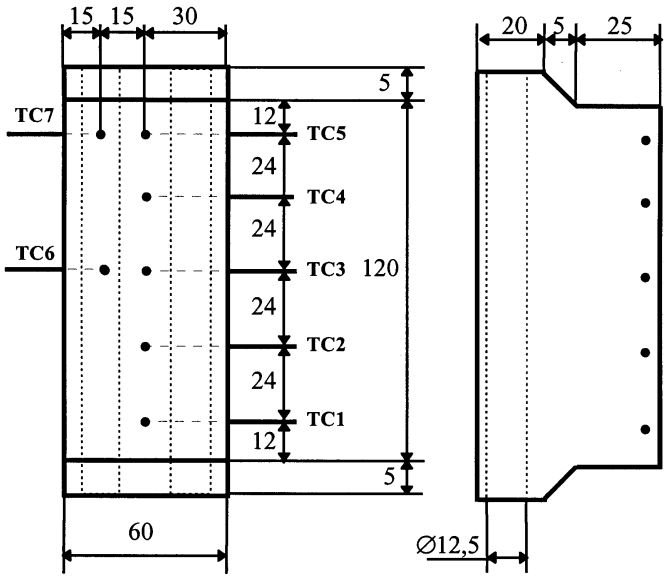

Fig. 2. Geometry of the copper block and location of the thermocouples (TCl,..., TC7) (dimensions in mm).

number 3 and 6 or 5 and 7 were identical, to check out that the temperature along the horizontal axis is uniform as indicated by the numerical simulation.

A hot-wire probe is placed at the center of the confined volume. In unconfined situation, it is located at the center of the heating plate, 1.25 mm from the surface in order to be in the middle of the vapor column whose thickness is about 2.5 mm according to Liaw and Dhir (1989).

The operating procedure has been described previously by Bonjour and Lallemand (1995). The boiling curves are plotted by decreasing heat flux in order to avoid hysteresis. The uncertainty on the heat flux is always lower than $\pm 1.3\%$ and the uncertainty on the mean wall superheat is always lower than ± 0.9 K.

2.2. Hot-wire anemometry technique for phase-detection

The equipment used for the hot-wire anemometry technique includes a CTA (constant temperature anemometer) model 1750 from TSI Inc. A tungsten–platinum coated wire (4 μm diameter and 0.125 mm long) is connected to the anemometer. The output signal of the anemometer is acquired by an acquisition card with a resolution of 5 mV and a conversion time of 25 μs. The sampling frequency is fixed at 2000 Hz and the sampling time at 6 s.

The anemometer mainly consists of a Wheatstone bridge, one leg of which is the hot-wire sensor. A secondary electronic circuit regulates the voltage necessary to keep the hot-wire at the operating temperature. Fig. 3 gives a typical evolution of the output signal as a function of time. When the sensor is immersed in the liquid, this voltage is high because of the efficient cooling of the wire. When it is in contact with vapor, the voltage is low because of the low heat transfer coefficient.

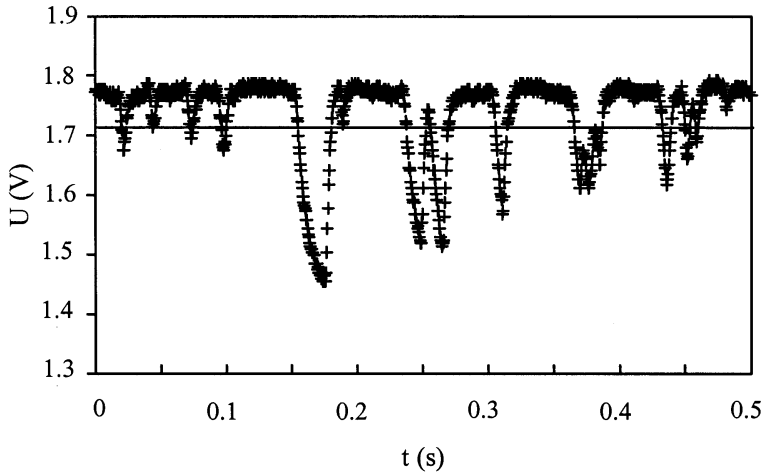

Fig. 3. Example of the CTA output signal as a function of time.

The operating temperature of the sensor and the phase-detection threshold value were determined from the procedure described by Carvalho and Bergles (1991). The optimum sensor superheat was found to be 68 K (i.e. a wire temperature of 115.6°C), which means that boiling of the fluid takes place on the hot wire. However, it has been pointed out by Carvalho and Bergles (1991) that this phenomenon implies few perturbations because the nature of the bubbles generated on the sensor is very different from that of the bubbles generated in the confined space. Indeed, the bubbles on the sensor have a very high frequency (200 Hz and more), a very low diameter (less than 50 μm according to photographic observations) and are generated very locally on the 125 μm long, 4 μm diameter wire. Their presence induces a 'boiling noise' (Toral, 1981) characterized by the high frequency oscillations of the voltage between the values $U = 1.74$ V and $U = 1.79$ V in Fig. 3. On the contrary, the bubbles generated on the heated wall have a frequency of about 0–100 Hz. Their diameters range from about 1 mm (isolated bubbles) to several centimeters (coalesced bubbles), indubitably corresponding to the large voltage variations. As regards the threshold, it was fixed at 1.71 V. So, in Fig. 3, each spike reaching a value lower than 1.71 V indicates a bubble passage. The beginning of a bubble passage is defined as the first point before a continuous decrease in the signal down to a voltage lower than 1.71 V. The end of a bubble passage corresponds to the last point after a continuous increase in the signal from a voltage lower than the threshold to a voltage greater than this threshold. A computer code has been written in order to evaluate the following parameters:

- the local time-averaged void fraction, which is defined as

$$\alpha = \frac{\sum t_{b,i}}{t_t}, \tag{3}$$

where $t_{b,i}$ is the passage time of the bubble number i and t_t the total sampling time;

- the bubble passage frequency

$$f_b = \frac{N}{t_t}, \tag{4}$$

where N represents the total number of bubble passages during t_t;

- the bubble mean passage time

$$t_b = \frac{\sum t_{b,i}}{N}. \tag{5}$$

From the bubble passage time distribution, bubble passages are classified into three categories : short passages, average passages and long passages. The contribution of a bubble category to the void fraction is defined as the ratio of the sum of the bubble passage times corresponding to this category to the sum of all the bubble passage times. This implies that the contribution of a bubble type to the void fraction is expressed as a percentage of the total void fraction. The analysis of each contribution allows a better knowledge of the two-phase flow structure.

3. Experimental Results and Discussion

3.1. Thermal performances and visual observations

Figure 4 shows boiling curves plotted for different gap-sizes. For low heat fluxes (lower than 3–5 W/cm^2), the wall superheat is reduced as the gap-size decreases, which indicates a heat transfer enhancement. However, for high heat fluxes, when the gap-size decreases, a heat transfer deterioration and a noticeable decrease in CHF occur. The whole experimental results concerning thermal performances of boiling in narrow spaces have been described in detail previously (Bonjour and Lallemand, 1995 ; Bonjour et al., 1996 ; Bonjour and Lallemand,

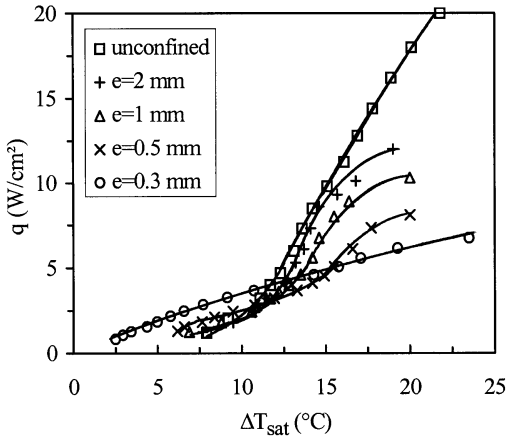

Fig. 4. Boiling curves obtained for various gap-sizes.

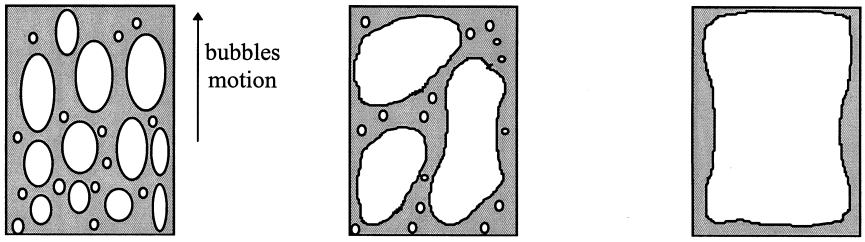

Fig. 5. Confined boiling regimes (front view).

1997; Bonjour et al., 1997). In those references, the fundamental mechanisms of the heat transfer enhancement at low heat flux have also been discussed. When bubbles are squeezed in the narrow channel, their microlayer (thin layer of liquid between the wall and the base of the bubble) is enlarged, which facilitates its evaporation and increases the latent heat transfer. The vapor of a bubble can also penetrate into neighboring nucleation sites, which makes nucleation easier. It has also been shown that, because of the presence of the confinement wall, the liquid in the channel is warmed-up more efficiently than in unconfined boiling. The thermal boundary layer is thicker and the nucleation process is enhanced. At least, one observes a higher liquid velocity in narrow channel than in unconfined situation, which allows a higher heat transfer coefficient.

During all the tests, we carefully observed the boiling regimes in the confined space with the naked eye. Three regimes have been identified (Fig. 5), but contrarily to the observations of Rampisela (1993), each regime was obtained for each confinement. At low heat fluxes, *boiling with isolated deformed bubbles* occurs. At moderate heat fluxes, the deformed bubbles gather together to form *coalesced bubbles*. When too many coalesced bubbles are generated at high heat fluxes, the heating surface is almost covered with a single mass of vapor, which characterizes the *partial dryout* regime. With a channel whose bottom and/or sides are closed, the decrease in CHF is more noticeable (Fujita, 1988) and the transitions between the regimes are expected to occur for lower heat fluxes than for the present geometry.

3.2. Hot-wire anemometry measurements

3.2.1. Void fraction measurements

The measured local void fraction is plotted as a function of the heat flux for $e = 0.5$, 1, 2 mm and ∞ (Fig. 6). For all the gap-sizes, void fractions increase with increasing heat flux since the amount of vapor becomes more and more important. For a given heat flux, a decrease in the channel gap-size increases the void fraction. Indeed, the confinement plate hinders the motion of the bubbles along the normal to the heated surface, which implies that all the bubbles generated below the hot-wire pass through the sensor. Moreover, an enhancement of nucleation occurs during confined boiling, which increases the amount of vapor generated in the channel.

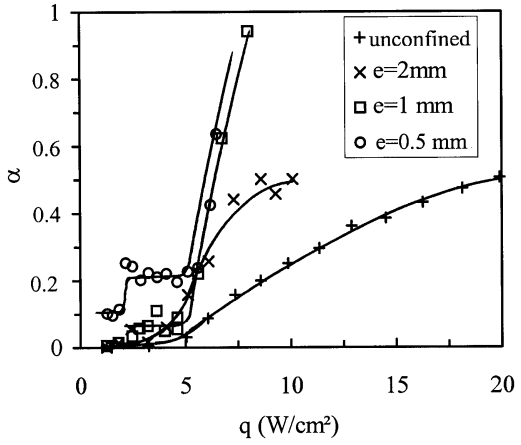

Fig. 6. Void fraction vs heat flux for various gap-sizes.

At low heat fluxes (<5 W/cm^2), for $e \geq 1$ mm, the void fraction is very low. The curve obtained for $e = 0.5$ mm shows two steps ($\alpha \approx 10\%$ for $q < 2$ W/cm^2 and $\alpha \approx 20\%$ for $2 < q < 5$ W/cm^2). In the former case, natural convection is the dominant heat transfer mode, whereas, in the latter case, bubbles are strongly deformed, so that the void fraction reaches a higher value. The steps correspond to a change in the regime as it will be shown later.

When CHF occurs, the void fraction is about 50% for large channels ($e = 2$ mm or ∞). This confirms the validity of Zuber et al. (1961) hydrodynamic theory for the triggering mechanism of CHF (coexistence of vapor and liquid 'jets'), that implies that CHF occurs for moderate void fractions since the heating surface is not completely blanketed by a vapor film. When the gap-size is too large to modify the distribution of the vapor jets, the main triggering mechanism of CHF is the hydrodynamic instability. But for narrow channels ($e = 0.5$ or 1 mm), CHF takes place when the heating surface is totally dried out ($\alpha \approx 80\%$–100%). These values are close to those obtained for CHF during forced convective boiling.

3.2.2. Measurements of bubble passage frequency

Figure 7 represents the frequency of bubble passages as a function of heat flux for various gap-sizes. For large channels ($e = 2$ mm or $e = \infty$), the frequency of bubble passages continuously increases from 1 to 3 bubble/s to 20 to 25 bubble/s when the heat flux increases from 1 W/cm^2 to CHF. However, for narrow channels ($e \leq 1$ mm), the frequency reaches a maximum corresponding to the dryout conditions characterized by a single large mass of vapor almost stable on the heating surface. Moreover, for $e = 0.5$ mm, at low heat fluxes, the frequency is larger (10 bubble/s) than for $e = 1$ mm (1 to 5 bubble/s). Indeed, when bubbles are squeezed and spread on the surface, the sensor can detect bubbles whose center can be laterally far away from the hot-wire.

3.2.3. Bubble passage time measurements

Figure 8 shows the influence of confinement on the mean passage time of the bubbles. This time always increases when the heat flux increases because bubbles become larger, whereas their rising velocity does not change much. For a given heat flux, when the channel gap-size is

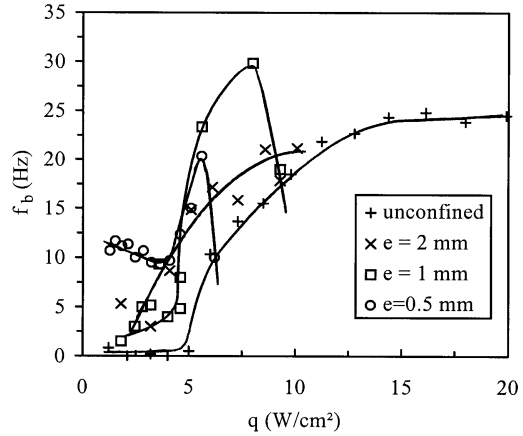

Fig. 7. Influence of heat flux and confinement on the bubble passage frequency.

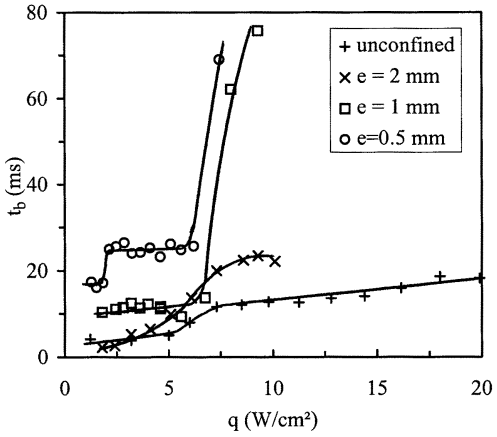

Fig. 8. Bubble passage time vs heat flux for various channel gap-sizes.

reduced, the mean passage time of bubbles is increased because they are squeezed. This trend is particularly noticeable for very narrow channels ($e \leq 1$ mm) at high heat fluxes, when the presence of coalesced bubbles and dryout lead to passage times up to seven times higher than for unconfined boiling. For $e = 0.5$ mm, two steps ($t_b = 18$ ms for $q < 2$ W/cm^2 and $t_b = 26$ ms for $2 < q < 6$ W/cm^2) appear, corresponding to those observed on Fig. 6.

3.2.4. Contribution of each bubble type to the void fraction

Figures 9–11 represent the contribution of the various types of bubbles (short for $t_{b,i} < 6$ ms, average for $6 < t_{b,i} < 14$ ms or long for $t_{b,i} > 14$ ms) to the void fraction as a function of the reduced heat flux (ratio of the heat flux to the CHF for the considered gap-size $q_{crit,e}$) for

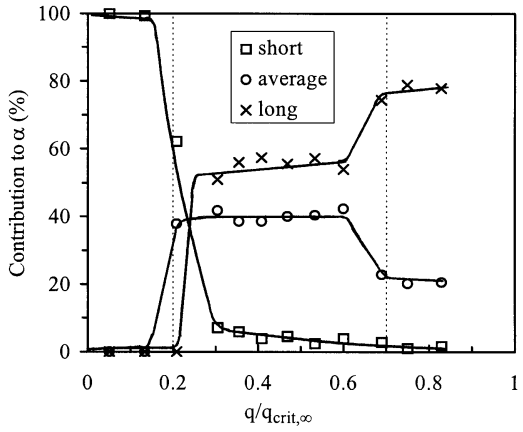

Fig. 9. Contribution of the various types of bubbles to the void fraction ($e = \infty$).

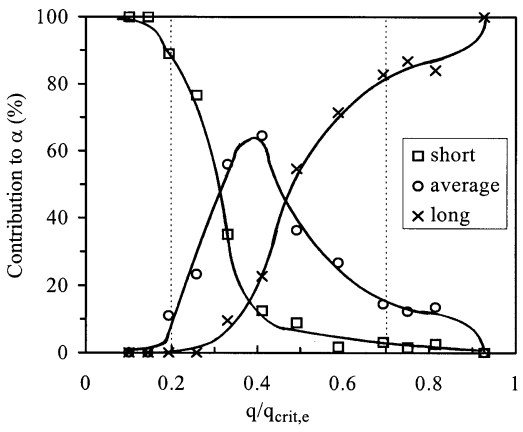

Fig. 10. Contribution of the various types of bubbles to the void fraction ($e = 2$ mm).

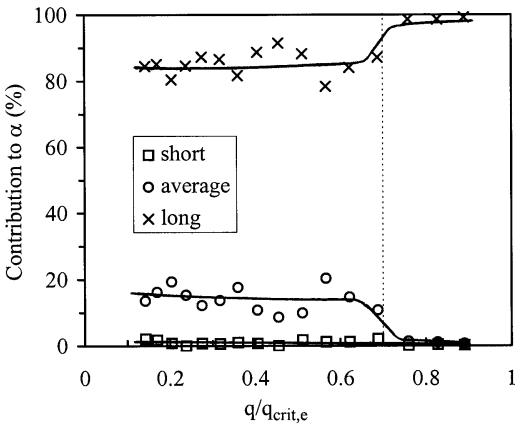

Fig. 11. Contribution of the various types of bubbles to the void fraction ($e = 0.5$ mm).

$e = \infty$, 1 mm and 0.5 mm, respectively. The curves obtained for $e = 2$ mm are very similar to those obtained for $e = 1$ mm.

For unconfined boiling (Fig. 9), three domains are clearly identified. For $q/q_{\text{crit,e}} < 0.2$, only bubbles with short passage times are present. They correspond to isolated bubbles observed by Gaertner (1965). For moderate heat fluxes ($0.2 < q/q_{\text{crit,e}} < 0.7$), the contribution of short bubbles is almost zero and the number of long and average bubbles is quite equivalent. In the vicinity of CHF ($q/q_{\text{crit,e}} > 0.7$), long bubbles [vapor mushrooms defined by Gaertner (1965)] are in the majority (80%).

For narrow channels such as $e = 1$ mm (Fig. 10), short bubbles represent 100% of the bubbles for low heat fluxes ($q/q_{\text{crit,e}} < 0.2$) and totally disappear for higher heat fluxes as for unconfined boiling. However, contrary to unconfined boiling, the contribution of long bubbles tends to 100% for $q/q_{\text{crit,e}} > 0.7$, which characterizes the dryout of the heating wall near CHF. For moderate heat fluxes ($0.2 < q/q_{\text{crit,e}} < 0.7$), the contribution of bubbles with average passage times reaches a maximum which is due to the competition between two phenomena. On the one hand, because of the confinement, the two-phase fluid velocity is increased. So, the passage time of a vapor mass is reduced and the mass may be counted as a short passage time bubble. On the other hand, the diameter of a vapor mass is increased with increasing heat flux, which implies an increase in its passage time for a given fluid velocity.

For $e = 0.5$ mm (Fig. 11), only two domains are clearly distinguished. For $q/q_{\text{crit,e}} < 0.7$, long bubbles are in the majority (80%) and the contribution of short bubbles is zero. Indeed, even at low heat fluxes, the bubbles are so squeezed that all of them are counted as bubbles of long or average passage time. For $q/q_{\text{crit,e}} > 0.7$, because of the dryout, all the bubbles have a long passage time. However, when plotting the bubble passage time as a function of the reduced heat flux for $e = 0.5$ mm (Fig. 12), it appears that the step corresponding to the transition between isolated deformed bubbles and coalesced bubbles also occurs for $q/q_{\text{crit,e}} = 0.2$ and the transition from coalesced bubbles to dryout for $q/q_{\text{crit,e}} = 0.7$. The high bubble mean passage time observed at low heat fluxes for $e = 0.5$ mm confirms that, even for this region, almost all the bubbles are long.

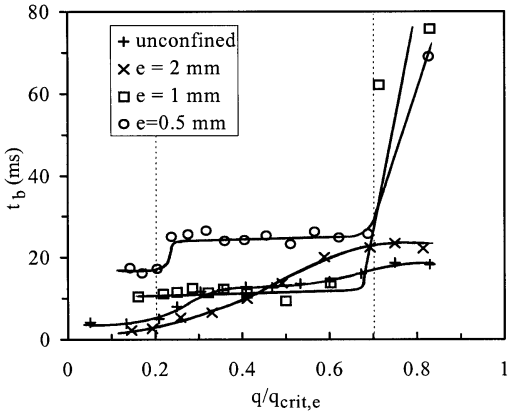

Fig. 12. Bubble passage time vs reduced heat flux for various channel gap-sizes.

3.2.5. Flow pattern map

The main characteristics of each flow pattern are shown in Table 1. From the graphs given in the previous section (Figs. 9–12), objective criteria for the transitions between the regimes in confined boiling have been determined. A boiling regime map is proposed for a confined space (Fig. 13) in terms of two dimensionless numbers: the Bond number [Eq. (1)] and the reduced heat flux relative to $q_{\mathrm{crit},\infty}$, i.e. CHF under unconfined conditions. The transition from isolated deformed bubbles to coalesced bubbles corresponds to $q/q_{\mathrm{crit,e}} = 0.2$ and that from coalesced bubbles to partial dryout to $q/q_{\mathrm{crit,e}} = 0.7$. The upper limit of the map represents the evolution of the ratio between the CHF for a given gap-size $q/q_{\mathrm{crit,e}}$ and $q_{\mathrm{crit},\infty}$ [both calculated with a correlation validated experimentally (Bonjour and Lallemand, 1997)]. Fig. 13 also shows a good agreement between our visual observations (points) and the domains defined by means of HWA (solid lines). One must however notice that discrepancies are probably due to the difficulty in visually identifying the regimes, particularly for very narrow channels ($Bo < 1$). On the contrary, the HWA technique provides objective transition criteria, even for $Bo < 1$. The

Table 1. Main characteristics of the confined boiling regimes (contributions of the various types of bubbles noted in brackets)

	Unconfined boiling ($e = \infty$)			Large channel (e = 2 or 1 mm)			Narrow channel (e = 0.5 mm)		
	α (%)	f_b (Hz)	bubble type	α (%)	f_b (Hz)	bubble type	α (%)	f_b (Hz)	bubble type
Isolated deformed bubbles	< 5	1	short (100%)	< 5	< 5	short (100%)	10	10	long (80%) average (20%)
Coalesced bubbles	5 to 40	10 to 25	long (55%) average (45%)	5 to 60	10 to 30	average (20–80%) long (20–80%)	10 to 60	10 to 30	long (80%) average (20%)
Partial dryout	40 to 50	25	long (80%)	60 to 100	low	long (100%)	60 to 100	low	long (100%)

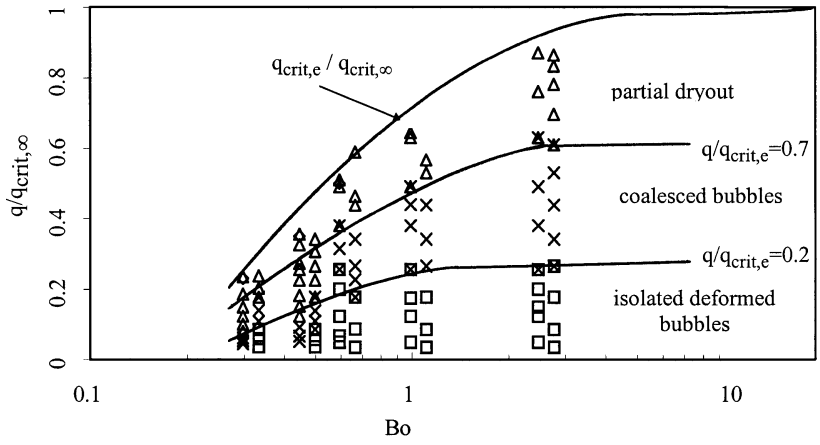

Fig. 13. Flow pattern map.

location of the regimes identified from HWA measurements are also compared to Rampisela (1993) visual observations (Fig. 14). A good agreement is found for nucleate boiling with coalesced bubbles. However, some observations of partial dryout or deformed bubbles do not seem to fit in with the domains defined by means of HWA. Indeed, the heating surface used by Rampisela (1993) consists of stacking five copper blocks which are heated independently, which implies that CHF occurs for a lower heat flux than in our experiment. At least, no comparison with other works has been made for narrow channels ($Bo < 1$), since it was not possible to find such information in the literature.

4. Conclusion

The aim of this work was to determine objective criteria for the transitions between confined boiling regimes (isolated deformed bubbles, coalesced bubbles, partial dryout) by means of hot-wire anemometry for phase detection. It is shown that this technique can provide meaningful

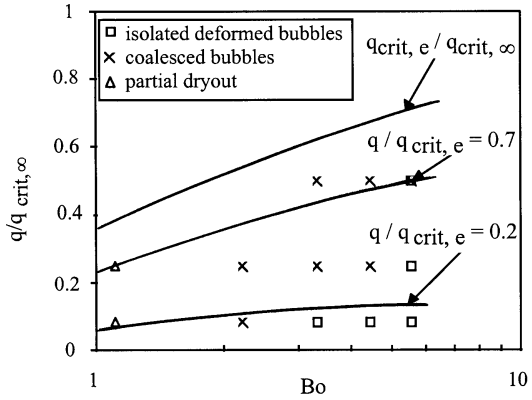

Fig. 14. Location of the regimes visualized by Rampisela (1993) on the proposed flow pattern map.

information concerning passage time and frequency of bubbles and void fraction. Moreover, by the study of the evolution of the contribution of various types of bubbles (short, average and long passage time bubbles) as a function of reduced heat flux, we show that the transition from isolated deformed bubbles occurs for $q/q_{\mathrm{crit,e}} = 0.2$ and that from coalesced bubbles to partial dryout for $q/q_{\mathrm{crit,e}} = 0.7$. So, we can propose a new flow pattern map that can be considered as particularly important when looking forward to proposing methods for the prediction of heat transfer coefficients for confined boiling for each regime.

References

Bonjour, J., Lallemand, M., 1995. Influence de la pression et du confinement sur les transferts thermiques au cours de l'ébullition convective naturelle. Revue Générale Thermique 34 (407), 667–677.

Bonjour, J., Zaghdoudi, M.C., Lallemand, M., 1996. Prediction of heat transfer coefficient during nucleate pool boiling in a vertical confined space. Eurotherm Seminar no 48 on Pool Boiling. Paderborn, Germany, pp. 201–208.

Bonjour, J., Lallemand, M., 1997. Effects of confinement and pressure on critical heat flux during natural convective boiling in vertical channels. International Communication on Heat and Mass Transfer 24 (2), 191–200.

Bonjour, J., Boulanger, F., Gentile, D., Lallemand, M., 1997. Etude phénoménologique de l'ébullition en espace confiné à partir d'un site de nucléation isolé. Revue Générale Thermique 36 (7), 562–572.

Carvalho, R.D.M., Bergles, A.E., 1991. The use of hot-wire anemometry for local void fraction measurements in pool boiling. 11th ABCM Mechanical Engineering Conference (XI COBEM) 1, 279–282.

Delhaye, J.M., 1969. Hot film anemometry in two-phase flow. 11th National ASME/AIChE Heat Transfer Conference: Two-Phase Flow Instrumentation , 58–69.

Elkassabgi, Y., Lienhard, J.H., 1987. Sidewall and immersion-depth effects on pool boiling burnout for horizontal cylindrical heaters. Journal of Heat Transfer 109, 1055–1058.

Fujita, Y., Ohta, H., Uchida, S., Nishikawa, K., 1988. Nucleate boiling heat transfer and critical heat flux in narrow space between rectangular surfaces. International Journal of Heat Mass Transfer 31 (2), 229–239.

Gaertner, R.F., 1965. Photographic study of nucleate pool boiling on a horizontal surface. Journal of Heat Transfer 2, 17–29.

Gentile, D., Zidat, S., 1992. Advanced engine cooling system. 24th FISITA Congress. London, UK, pp. 215–222.

Herringe, R.A., Davis, M.R., 1974. Detection of instantaneous phase changes in gas–liquid mixture. Journal of Physics E: Scientific Instruments 7, 807–812.

Hsu, Y.Y., Simon, F.F., Graham, R.W. 1963. Application of hot wire anemometry for two-phase flow measurements such as void fraction and slip velocity. ASME Winter Meeting : Multiphase Flow Symposium. 26–34. Philadelphia.

Jomard, T., Eckes, U., Touvier, E., Lallemand, M. 1992. Modeling of the two-phase cooling of a power semiconductor and its evaporator. 8th Annual IEEE SEMI-THERM. 6. Austin, TX.

Liaw, S.P., Dhir, V.K., 1989. Void fraction measurements during saturated pool boiling of water on partially wetted vertical surfaces. Journal of Heat Transfer 111, 731–738.

Monde, M., Kusuda, H., Uehara, H., 1982. Critical heat flux during natural convective boiling in vertical rectangular channels submerged in saturated liquid. Journal of Heat Transfer 104, 300–303.

Rampisela, P.F., 1993. Etude expérimentale de l'ébullition en espace confiné. Thèse de Doctorat. INPG, Grenoble, France, p. 193.

Toral, H., 1981. A study of the hot-wire anemometer for measuring void fraction in two phase flow. Journal of Physics E: Scientific Instruments 14, 822–827.

Westwater, J.W., Hwalek, J.J., Irving, M.E., 1986. Suggested standard methods for obtaining boiling curves by quenching. Industrical Engineering and Chemistry Fundamentals 25, 685–692.

Xia, C., Guo, Z., Hu, W., 1992. Mechanism of boiling heat transfer in narrow channels. San Diego, CA 197, 111–119.

Yao, S.C., Chang, Y., 1983. Pool boiling heat transfer in a confined space. International Journal of Heat and Mass Transfer 26 (6), 841–848.

Zuber, N., Tribus, M., Westwater, J.W. 1961. The hydrodynamic crisis in pool boiling of saturated and subcooled liquids. International Developments in Heat Transfer. 230–236. ASME, New York.